III-V Thin-Film Solar Cells Bonded to Si Substrates via Metal Grids

ECS Transactions, 98 (4) 117-123 (2020)
10.1149/09804.0117ecst ©The Electrochemical Society

III-V Thin-Film Solar Cells Bonded to Si Substrates via Metal Grids

T. Hishida[a], J. Liang[a], and N. Shigekawa[a]

[a] Graduate School of Engineering, Osaka City University, Osaka 558-8585, Japan

Using surface-activated bonding technologies, we bond InGaP/GaAs double-junction (2J) solar-cell structures invertedly-grown on GaAs substrates to metal grids formed on conductive Si substrates. The metal grids are made of 170-nm SiO_2 layers and 310-nm Ti/Au metal layers. 2J cells are fabricated by eliminating the GaAs substrates and forming emitter and base contacts. The emitter contacts are aligned to the metal grids. The fabricated 2J cells reveal a lower series resistance in comparison with cells directly bonded to Si substrates, which is likely to be due to a lower resistance across GaAs//metal grid junctions than that across GaAs//Si junctions. A higher open-circuit voltage and a larger internal quantum efficiency are also observed for the 2J cells on metal grids. These features as well as the oscillation in reflectance spectrum suggest that the 2J cells work as optically-isolated thin-film cells.

Introduction

Among a variety of solar-cell configurations, multijunction (MJ) cells made of stacks of subcells with different bandgaps are promising as key devices in next-generation photovoltaics (1). High efficiencies are assumed to be realized with low process costs by integrating upper-part subcells of III-V compound semiconductors and Si-based bottom cells into III-V-on-Si MJ cells (2–12). The wafer bonding of dissimilar materials (13, 14) such as surface-activated bonding (SAB) (15), i.e., the hybrid approach has been applied for fabricating III-V-on-Si MJ cells because of difficulties in hetero-epitaxial growth of III-V subcell layers on Si.

In SAB, surfaces of substrates to be bonded are activated using a fast atom beam (FAB) of Ar so that they are bonded without heating. The irradiation of Ar FAB simultaneously introduces midgap states at the bonding interfaces and causes a large interface resistance (16). It was found that a post-bonding annealing played a role of decreasing the interface resistance (12, 17). A resistance as low as ~2 $m\Omega cm^2$ was obtained for n^+-GaAs//n^+-Si junctions when they were annealed at 300 ℃ for 1 h (12). In actual hybrid MJ cells, however, thin bonding layers of Si bottom cells, which also work as emitter layers, are depleted when the surfaces of bottom cells are irradiated by the Ar FAB. The series resistance, consequently, is still apparent even after the junctions are annealed.

A solution for this problem is to passivate the surface of Si bottom cells by transparent conductive materials. One approach based on such concept is the use of bottom cells with TOPCON structures (9, 11). It is assumed that the range of optimum

thickness of SiO_2 tunnelling passivation layers is narrow since the SiO_2 layers are etched by the FAB irradiation. Indium tin oxide (ITO) layers were used as intermediate layer between III-V and Si subcells, which played a role of decreasing the series resistance of III-V-on-Si hybrid MJ cells (10). It was found that the mismatch in photo currents between III-V and Si subcells was enhanced by using ITO layers because of their free-carrier absorption. We also observed the increase of resistance in junctions with ITO layers when they were annealed (18).

We deposited SiO_2 layers on surfaces of Si substrates. We then formed comb-shaped metal grids by etching the SiO_2 layers, evaporating contact metals and lift-off. The metal layers were thicker than the SiO_2 layers. Using SAB, we fabricated Si//metal grid/Si and GaAs//metal grid/Si junctions in which Si or GaAs substrates were connected to the surface of metal layers. These junctions revealed a lower resistance than the resistance of junctions with intermediate ITO layers when they were annealed (19). In this work, we bond GaAs epi substrates to Si substrates via metal grids and fabricate InGaP/GaAs 2J cells on Si substrates by applying the device process sequence.

Results and Discussions

Cell Fabrication

We deposited 170-nm thick SiO_2 layers on conductive Si substrates by using RF magnetron sputtering. After etching the SiO_2 layers we fabricated comb-shaped metal grids by electron-beam evaporation of Ti/Au layers and lift-off. The total thickness of metal layers was 310 nm so that the air gap between the bonded 2J structures and SiO_2 layers was assumed to be 140 nm. The width and gap of metal grids were 20 and 180 μm, respectively. The coverage of metal layers over Si substrates was 25%. Then we bonded InGaP/GaAs 2J structures that were invertedly grown on GaAs substrates to the metal grids using SAB technologies. The thickness of 2J structures was nominally 4.4 μm. The junctions were heated at 200 ℃ for 1 h in a bonding chamber while a pressure of 30 MPa was applied. Details of the bonding process were previously reported (19).

Next the GaAs substrates were eliminated using selective wet etching. On the exposed n^+-doped GaAs contact layers we made emitter contacts aligned to the metal grids by evaporating Ti/Au and lift-off. The contact layers that were not covered by the emitter contacts were selectively etched off. The base contacts were formed on the backside of Si substrates. The cell area (3.5 mm^2) was defined by dicing, so that the fabrication process was completed. Note that the cell was not coated with an anti-reflection (AR) film. The schematic process flow as well as a top view of bonded 2J structures after forming emitter contacts are shown in Figs. 1(a) and 1(b), respectively. A scanning electron microscope (SEM) image of the cross section of junctions at metal grids is shown in Fig. 1(c), which indicates that the emitter contacts were aligned to the metal grids.

Cell Characteristics

Using an in-house solar simulator, we measured the current-voltage (*I-V*) characteristics of the fabricated cell under an air mass 1.5G/one sun solar irradiance. The

characteristics are shown in Fig. 2. The shadow loss due to the emitter contacts was not compensated for. The characteristics of a 4-mm^2 AR-coated InGaP/GaAs 2J cell with the same layer structure that was directly bonded to a Si substrate are also shown for comparison (4). Their short-circuit currents, open circuit voltages, series resistances, shunt resistances, and conversion efficiencies are summarized in Table I. We also measured the spectral response of the cell. The observed external quantum efficiency (EQE), reflectance, and internal quantum efficiency (IQE) are shown in Fig. 3(a). A previously-reported spectral response of 2J cells directly bonded to Si substrates (10) is shown in Fig. 3(b) for comparison.

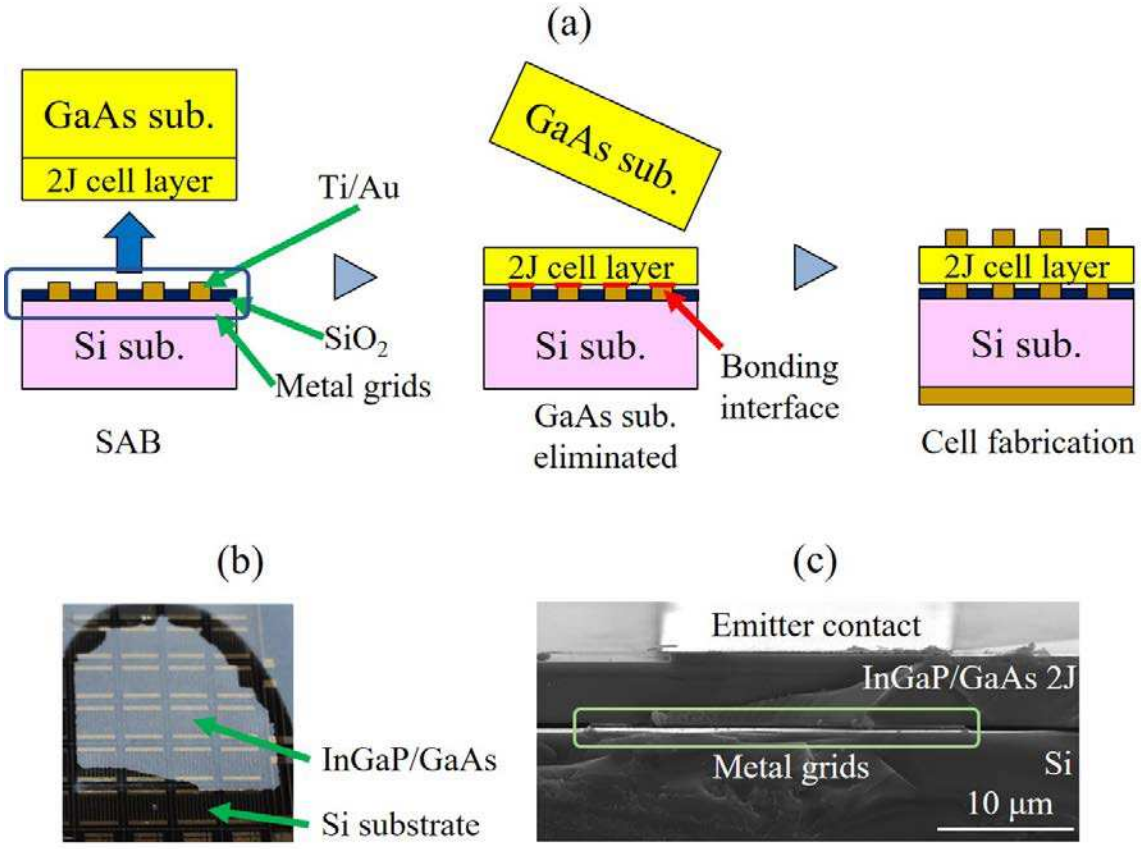

Figure 1. (a) Schematic process flow for fabricating III-V cells bonded to Si substrates via metal grids. (b) A top view of bonded III-V 2J layers after forming emitter contacts. (c) A cross-sectional SEM image of InGaP/GaAs//metal grid/Si junctions.

The series resistance of the 2J cell on metal grids is lower than the resistance of the directly-bonded cell. The difference in resistance is likely to be due to a lower resistance across the bonding interfaces in junctions with metal grids (19). We also find that the 2J cell on metal grids reveals a higher open-circuit voltage (2.47 V) and a larger IQE (90 and >95% at maximum for the InGaP and GaAs subcells, respectively) than the directly-bonded cell (an open-circuit voltage of 2.16 V and an IQE of 80 and 90% at maximum for the InGaP and GaAs subcells, respectively). In contrast, the short-circuit current and EQE of the 2J cell on metal grids are lower than those of the directly-bonded 2J cell, which is attributable to the lack of AR coatings in the cell on metal grids.

Optical Resonance in 2J Cells

The oscillatory features in reflectance spectra suggest the occurrence of optical resonance. A simple analysis indicates that the oscillation of reflectance of the cell on metal grids between 900 and 1100 nm is due to the resonance in a 4.7-μm film with the refractive index of GaAs (20). Noting that the estimated thickness is close to the nominal thickness of 2J structures (4.4 μm), we assign the observed oscillation to the resonance in the entire 2J cell. This means that the 2J cell is optically separated from the Si substrate, i.e., it works as thin-film cell (21). The higher IQE and larger open-circuit voltage of the 2J cell on metal grids might be explained in this scheme.

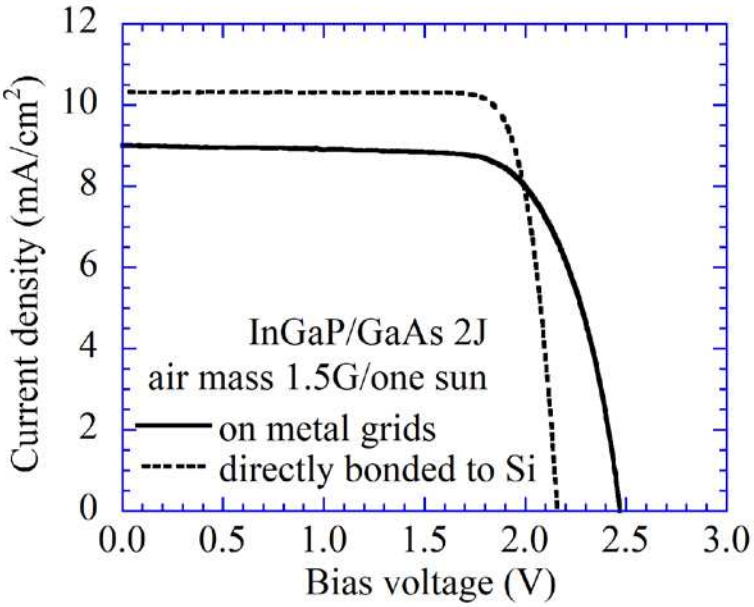

Figure 2. *I-V* characteristics of an InGaP/Si 2J cell bonded via metal grids under an air mass 1.5G/one sun solar irradiance. *I-V* characteristics of a 2J cell directly-bonded to a conductive Si substrate (ref. 4) are also shown.

Table I. Characterististics of a InGaP/GaAs 2J cell bonded via metal grids to Si. Characteristics of a 2J cell directly-bonded to Si (ref. 4) are also shown for comparison.

	InGaP/GaAs 2J cell	
	Bonded via metal grids	**Directly bonded to Si**
Short-circuit current (mA/cm^2)	9.0	10.3
Open-circuit voltage (V)	2.47	2.16
Conversion efficiency (%)	16.1	18.4
Fill factor	0.72	0.83
Series resistance (Ωcm^2)	1.82	11.0
Shunt resistance (Ωcm^2)	1.54×10^4	2.61×10^6

The operation of Si bottom cells of InGaP/GaAs/Si 3J cells is due to the incident light with a limited wavelength range of 900-1100 nm. The generated current in the Si bottom cells is, consequently, smaller than the currents generated in the InGaP top cells and GaAs middle cells. A high reflectance of the 2J cell on metal grids in this wavelength range (~60%), which is attributed to the optical properties of structures between III-V

layers and Si substrates, must be lowered in applying the bonding via metal grids for fabricating III-V-on-Si MJ cells. We calculated the power of photons transmitted to Si underneath by using the photon spectrum of air mass 1.5G and one sun. Dependencies of the ratio of the transmitted power to the power of incident photons on the thickness of SiO_2 layers and the gap between 2J cells and SiO_2 layers are shown in Fig. 4. The ratio is 50-60% for the case of a 170-nm SiO_2 layer and a 140-nm air gap. A higher optical power is assumed to be transmitted to Si bottom cells by optimizing the structure of passivating films and the air gap.

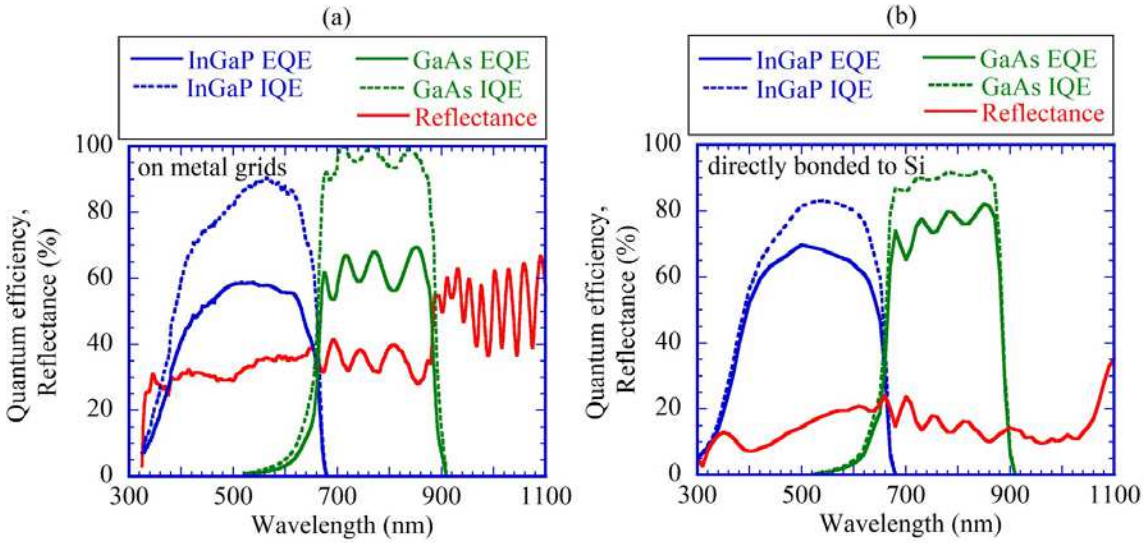

Figure 3. The external quantum efficiency, internal quantum efficiency, and reflectance of (a) an InGaP/GaAs 2J cell bonded via metal grids to Si substrate and (b) 2J cell directly bonded to Si substrate (ref. 10).

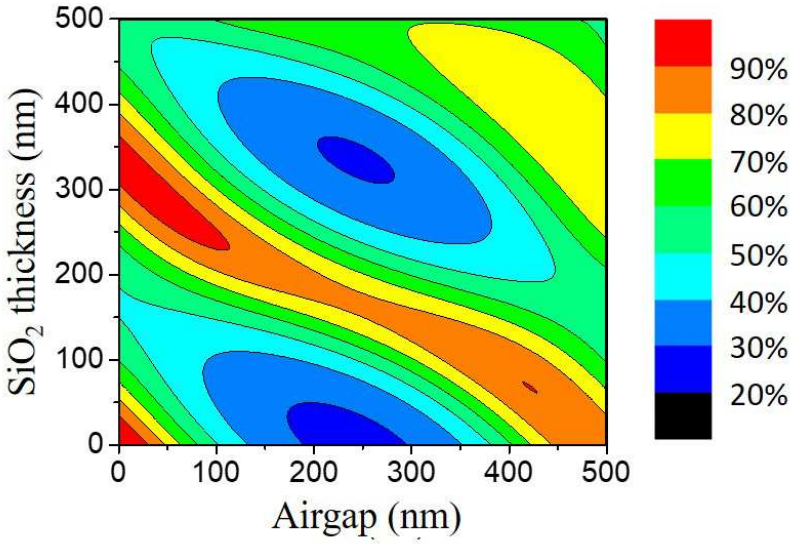

Figure 4. Dependencies of the ratio of optical power transmitted to Si to the incident power on the thickness of SiO_2 layers and the air gap between 2J cells and SiO_2 layers.

Conclusions

We successfully fabricated InGaP/GaAs double-junction (2J) cells on metal grids, which were composed of SiO_2 films for passivation and metal layers formed on Si substrates, by bonding the 2J epi substrates to metal grids, eliminating the GaAs substrates, and applying the semiconductor device process. The fabricated 2J cell revealed a larger open-circuit voltage, a lower series resistance, and a higher internal quantum efficiency (IQE) in comparison with a 2J cell directly bonded to Si. The difference in series resistance was attributed to a lower interface resistance of junctions made of metal grids. The larger open-circuit voltage and higher IQE of the cell on metal grids suggested that it works as optically-isolated thin-film cell, which explained the oscillatory features of the reflectance spectrum of the cell on metal grids. It was pointed out that the structure of passivating films and the air gap between the III-V layers and passivating films should be optimized in applying the metal-grid bonding for fabricating hybrid multijunction cells.

Acknowledgments

The epi substrates used in this work were grown at Sharp Corporation. This work was supported by the “Research and Development of ultra-high efficiency and low-cost III-V compound semiconductor solar cell modules (High efficiency and low-cost III-V/Si tandem)” project of New Energy and Industrial Technology Development Organization (NEDO). A part of this work was supported by Kyoto University Nano Technology Hub in “Nanotechnology Platform Project” sponsored by the Ministry of Education, Culture, Sports, Science and Technology (MEXT), Japan.

References

1. M. A. Green, E. D. Dunlop, D. H. Levi, J. H.-Ebinger, M. Yoshita, and A. W. Y. H.-Baillie, *Prog. Photovolt., Res. Appl.*, **27**, 565 (2019).
2. K. Derendorf, S. Essig, E. Oliva, V. Klinger, T. Roesener, S. P. Philipps, J. Benick, M. Hermle, M. Schachtner, G. Siefer, W. Jäger, and F. Dimroth, *IEEE J. Photovoltaics*, **3**, 1423 (2013).
3. N. Shigekawa, M. Morimoto, S. Nishida, and J. Liang, *Jpn. J. Appl. Phys.*, **53**, 04ER05 (2014).
4. N. Shigekawa, L. Chai, M. Morimoto, J. Liang, R. Onitsuka, T. Agui, H. Juso, and T. Takamoto, in *Proc. 40th IEEE Photovoltaic Specialists Conference*, p. 534, IEEE, Piscataway, NJ (2014).
5. S. Essig, J. Benick, M. Schachtner, A. Wekkeli, M. Hermle, and F. Dimroth, *IEEE J. Photovoltaics*, **5**, 977 (2015).
6. N. Shigekawa, J. Liang, R. Onitsuka, T. Agui, H. Juso, and T. Takamoto, *Jpn. J. Appl. Phys.*, **54**, 08KE03 (2015).
7. R. Cariou, J. Benick, P. Beutel, N. Razek, C. Flötgen, M. Hermle, D. Lackner, S. W. Glunz, A. W. Bett, M. Wimplinger, and F. Dimroth, *IEEE J. Photovoltaics*, **7**, 367 (2017).

8. S. Essig, C. Allebé, T. Remo, J. F. Geisz, M. A. Steiner, K. Horowitz, L. Barraud, J. S. Ward, M. Schnabel, A. Descoeudres, D. L. Young, M. Woodhouse, M. Despeisse, C. Ballif, and A. Tamboli, *Nat. Ene.*, **2**, 17144 (2017).
9. R. Cariou, J. Benick, F. Feldmann, O. Höhn, H. Hauser, P. Beutel, N. Razek, M. Wimplinger, B. Bläsi, D. Lackner, M. Hermle, G. Siefer, S. W. Glunz, A. W. Bett, and F. Dimroth, *Nat. Ene.*, **3**, 326 (2018).
10. N. Shigekawa, T. Hara, T. Ogawa, J. Liang, T. Kamioka, K. Araki, and M. Yamaguchi, *IEEE J. Photovoltaics*, **8**, 879 (2018).
11. D. Lackner, O. Höhn, R. M¨uller, P. Beutel, P. Schygulla, H. Hauser, F. Predan, G. Siefer, M. Schachtner, J. Schön, J. Benick, M. Hermle, and F. Dimroth, *Solar RRL*, DOI: 10.1002/solr.202000210
12. N. Shigekawa, R. Kozono, S. Yoon, T. Hara, J. Liang, and A. Yasui, *Sol. Energy Mater. Sol. Cells*, **210**, 110501 (2020).
13. O. Moutanabbir and U. Gösele, *Annu. Rev. Mater. Res.*, **40**, 469 (2010).
14. K. Tanabe, K. Watanabe, and Y. Arakawa, *Scientific Reports*, **2**, 349 (2012).
15. H. Takagi, K. Kikuchi, R. Maeda, T. R. Chung, and T. Suga, *Appl. Phys. Lett.*, **68**, 2222 (1996).
16. M. Morimoto, J. Liang, S. Nishida, and N. Shigekawa, *Jpn. J. Appl. Phys.*, **54**, 030212 (2015).
17. S. Essig and F. Dimroth, *ECS J. Solid State Science and Technol.*, **2**, Q178 (2013).
18. T. Hara, T. Ogawa, J. Liang, K. Araki, T. Kamioka, and N. Shigekawa, *Jpn. J. Appl. Phys.*, **57**, 08RD05 (2018).
19. T. Hishida, J. Liang, and N. Shigekawa, *Jpn. J. Appl. Phys.*, 59, SBBB04 (2020).
20. J. S. Blakemore, *J. Appl. Phys.*, **53**, R123 (1982).
21. T. Nakata, K. Watanabe, N. Miyashita, H. Sodabanlu, M. Giteau, Y. Nakano, Y. Okada, and M. Sugiyama, *Jpn. J. Appl. Phys.*, **57**, 08RF03 (2018).